

# MEASUREMENT OF STABILITY DIAGRAM AT IOTA AT FERMILAB\*

M.K. Bossard<sup>†</sup>, Y.-K. Kim, The University of Chicago, Chicago, IL, USA

R. Ainsworth, N. Eddy, O. Mohsen, Fermi National Accelerator Laboratory, Batavia, IL, USA

## Abstract

Nonlinear focusing elements can enhance the stability of particle beams in high-energy colliders by means of Landau Damping, through the tune spread which is introduced. We propose an experiment at Fermilab's Integrable Optics Test Accelerator (IOTA) to investigate the influence of nonlinear focusing elements on the transverse stability of the beam. In this experiment, we employ an anti-damper, an active transverse feedback system, as a controlled mechanism to induce coherent beam instability. By utilizing the anti-damper, we can examine the impact of the nonlinear focusing element on the beam's transverse stability. The stability diagram, a tool used to determine the system's stability, will be measured using a recently demonstrated method at the LHC. This measurement is carried out experimentally by selecting specific threshold gains and measuring them for a range of phases. The experiment at IOTA adds insight towards the stability diagram measurement method by supplying a reduced machine impedance, to investigate the impedance's effect on the stability diagram, as well as a larger range of phase measurements.

## MOTIVATION

Landau damping (LD) is the damping of the collective oscillation modes. In particle accelerators, Landau damping occurs due to the inherent variation in the betatron and synchrotron frequencies within the beam. Without Landau damping, intense particle beams would become unstable due to various collective unstable modes. These modes would negatively impact the quality of the beam in both its transverse and longitudinal directions. Therefore, understanding the magnitude of Landau Damping is crucial for predicting the stability of high-energy colliders.

Landau damping studies are commonly approached via stability diagram theory. Given the collective motion frequency  $\Delta\omega$ , the frequency in the presence of LD  $\Omega$  is given by the following relation [1]:

$$\Delta\omega = -1 / \int \frac{J_x \partial F / \partial J_x}{\Omega + \delta\omega(J_x + J_y) + i\omega} dJ_x dJ_y, \quad (1)$$

where  $F(J_x, J_y)$  is the beam's unperturbed distribution function,  $\delta\omega$  is the action-dependent frequency shift, and  $i\omega$  is a negligible imaginary number. To find  $\Omega$ , one would need to solve Eq. (1) for all  $\Delta\omega$ . From this, a stability contour would be produced in the  $\Delta\omega$  space when  $\text{Im}\Omega = 0$ . Often to find the stability diagram, one would use beam transfer function

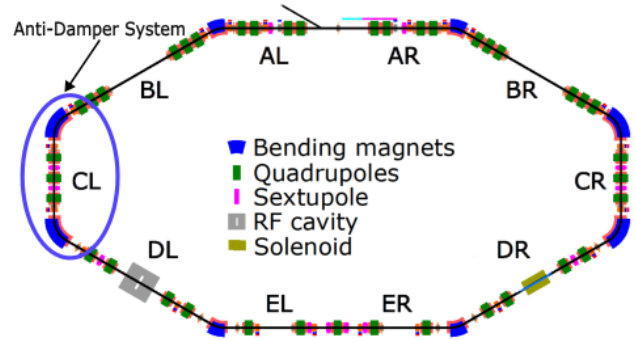


Figure 1: Schematic of the Integrable Optics Test Accelerator (IOTA). The anti-damper system elements are located in section CL, as circled in the figure.

(BTF) measurements through the frequency dependence of the response to forced beam oscillations.

There are limitations to the BTF method for obtaining stability diagrams, including that the measurement does not probe the actual strength of Landau damping but rather the BTF, and therefore relies on assumptions in Eq. (1). These assumptions include that the spread of synchrotron frequency is negligible, the beam response to external excitations is linear, that the betatron frequency spread is sufficiently small, and that the coherent modes are uncoupled [1]. As there are multiple sources for error in the BTF method to obtain stability diagrams, an alternative method has been proposed by Alexey Burov. As proof-of-principle it has been initially studied at the LHC [1] using an anti-damper, and is now further being studied and quantified at the Integrable Optics Test Accelerator (IOTA) at Fermilab.

IOTA, shown in Fig. 1, is a 40 m re-configurable ring dedicated towards research of accelerator physics and beam dynamics. IOTA can circulate both electrons and protons, where this experiment is for when electrons are circulating. This experiment aims to measure the stability diagram using an anti-damper, where an anti-damper is an active feedback system, used as a controllable source of beam impedance.

## METHODS

The IOTA transverse feedback system consists of a digital controller, a stripline kicker, two stripline BPMs, and a BPM analog module. A schematic of the experimental setup can be seen in Fig. 2.

The digital controller allows one to vary both the gain and the phase of the system. This provides the means to measure the full stability diagram. The beam first gets kicked by the kicker, where the total phase from the two BPMs is adjusted to supply the correct phase change as a virtual pickup. Once these elements are adjusted to produce the correct impedance, the stripline BPMs measure the beam

\* Work supported by The University of Chicago and Fermi National Accelerator Laboratory

<sup>†</sup> mbossard@uchicago.edu

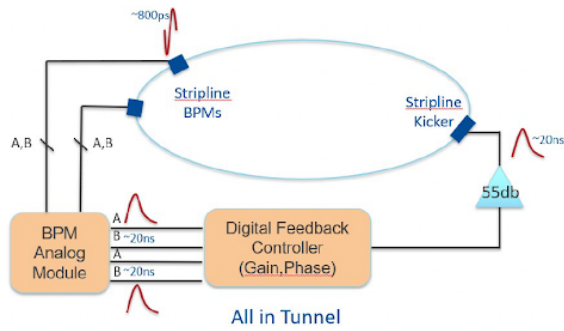


Figure 2: Schematic of Experimental Setup in the IOTA ring.

position. The two pickups are approximately  $110^\circ$  in phase advance apart, so both the position and velocity of the beam can be measured in a single turn. The results are then used to adjust the gain or phase until an instability is observed.

The experimental process includes measuring the stability diagram for a range of Landau octupole strengths in IOTA. In order to perform these stability diagram measurements, the anti-damper, composed of the stripline pickups and kicker, is employed to incite the instabilities. The anti-damper supplies a constant wake force on the beam  $\omega(z) = \text{constant}$ , where the resulting impedance goes as:

$$Z(\omega) \propto g e^{i\phi} \delta(\omega), \quad (2)$$

where  $g$  is the initial growth rate at instability and  $\phi$  is the phase between the kicker and the virtual pickup. This coupling impedance shifts the frequencies of collective modes by:

$$\Delta\omega \propto -ige^{i\phi}. \quad (3)$$

By independently adjusting the gain and phase delay between the pickups and kicker, one can set the feedback transfer anywhere in the complex plane, thus giving a source of controlled impedance.

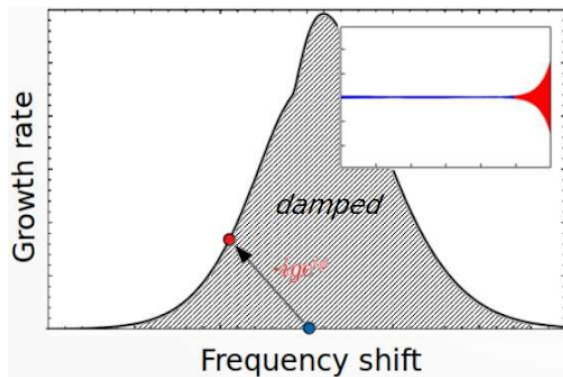


Figure 3: Theoretical Stability diagram. The beam is considered damped by Landau damping under the curve [2].

For a given gain one can observe at what feedback phase the beam becomes unstable. The growth rate of the unstable beam can be observed and mapped to a stability diagram, which presents the growth rate as a function of the collective mode frequency  $\Delta\omega$ , as is theoretically presented in Fig. 3. The stability diagram can also be presented as the imaginary

part of the frequency shift as a function of the real part of the frequency shift.

Before data-collection, the system was first calibrated in order to know the correspondence between the bpm coefficients and the phase advance. To do this, the bpm1 and bpm2 coefficients were both set to 1. A frequency sweep was performed for both the lower and upper sidebands, ranging from  $5.15 \cdot 10^6 - 5.35 \cdot 10^6$  Hz and  $9.65 \cdot 10^6 - 9.85 \cdot 10^6$  Hz, respectively. For each of these sweeps, a beam transfer function was obtained and the phase at the maximum BTF magnitude was recorded. An image of a BTF scan can be seen below in Fig. 4.

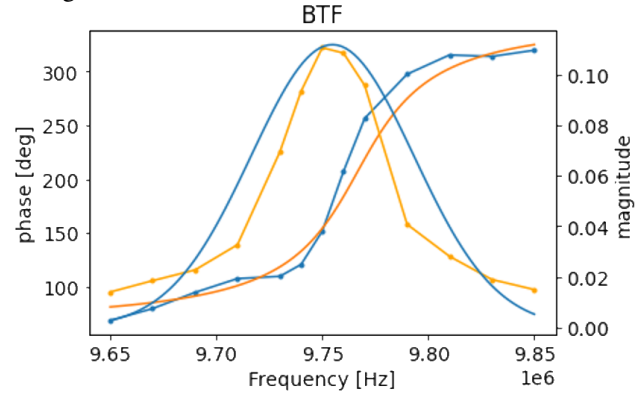


Figure 4: Example BTF measurement. The phase at the frequency peak corresponds to the experimental phase advance for the sideband.

The difference between the two sideband phases is related to the phase from the virtual pickup to the kicker as [3]:

$$\theta_{lsb} - \theta_{usb} + 180 = 2\phi, \quad (4)$$

where the addition of  $180^\circ$  is to account for the notch filter used by the board, as it attains the difference between revolutions rather than the total difference.

Plotting the phase advance as a function of the bpm coefficients results in Fig. 5. From this figure, a correspondence between the pickup-kicker phase and the bpm coefficients is obtained.

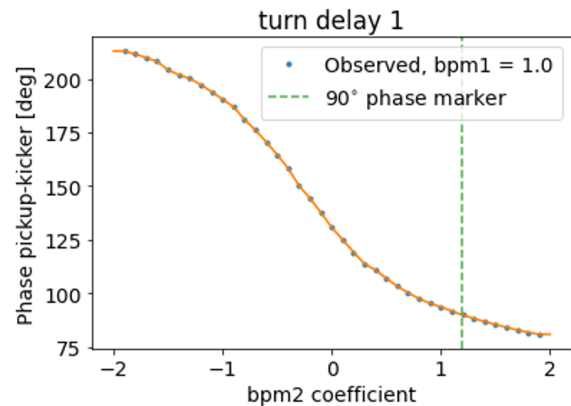


Figure 5: Phase advance as function of the bpm2 coefficient. The bpm1 coefficient was set to 2.0 for all points. The  $90^\circ$  marker shows the bpm2 coefficient which produces maximum instability.

Therefore, when experimental data is collected for different bpm coefficients, the corresponding phase advance can be determined.

## EXPERIMENTAL RESULTS

The first experimental goal was to incite an instability with a 90° phase advance from the virtual pickup to kicker, as 90° is the phase which should supply the most unstable motion. Once an initial instability was observed, a sweep over kicker gain and phase was performed. For each phase advance between the pickup and the kicker, a range of kicker gains was swept through. Once the kicker gain was large enough to create an instability, the growth rate of that instability was recorded. For the first set of experiments, a growth rate was detected when the beam position reached approximately 1500 position × intensity. Once an instability was detected, an exponential fit was performed on the envelope of the beam's centroid position. An example of the exponential fitting can be seen in Fig. 6. From this image, it can be seen that an instability has been incited and a growth rate of the beam's position envelope obtained.

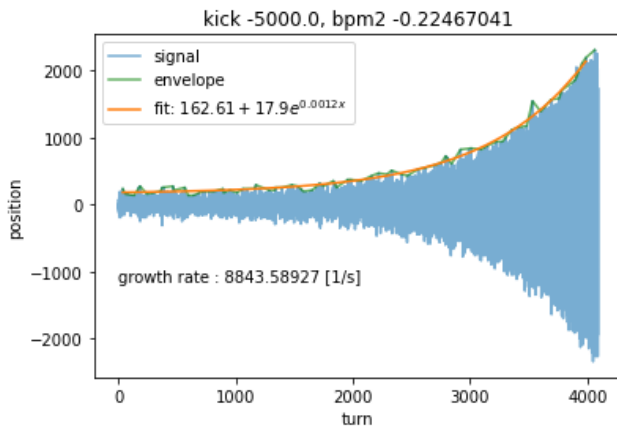


Figure 6: Growth rate of the beam centroid position. Exponential fit is performed on the envelope. This growth is for a kick gain setting of -5000 and a bpm coefficients of 2.0 and -0.22 for bpm1 and bpm2, respectively.

For a range of phases and kicker gain variations, growth rates were obtained. By plotting the growth rates for different kicker gains as a function of the experimental kick, the kicker gain multiplied by the beam current, linear fits were obtained and extrapolated. Such a linear fit for various bpm2 coefficients and sweeps of kicker gain can be seen in Fig. 7. This was performed for a ring turn delay of 1. From the linear fits, the fitted initial growth rate for a certain experimental kick can be obtained. This will be used as the growth rate for the stability diagram. By using this initial growth rate and by using Eq. (3), the frequency shift for each growth rate and phase combination can then be obtained. By plotting the imaginary part of the frequency shift as a func-

tion of the real part, the stability diagram can be achieved.

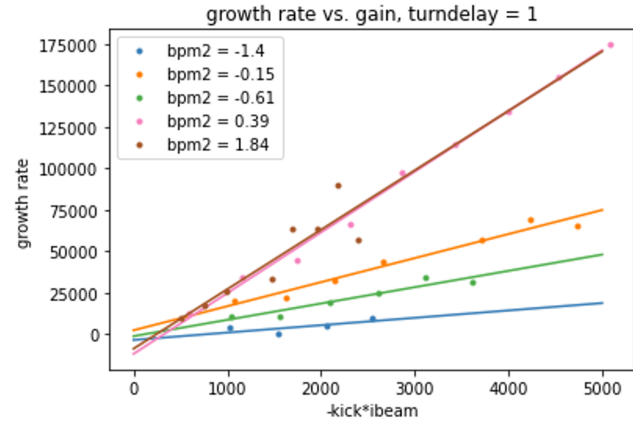


Figure 7: Stability Diagram obtained in IOTA with a growth rate threshold of 1500.

## CONCLUSIONS AND NEXT STEPS

This experiment is well-commissioned and prepared to take larger sets of data for stability diagrams. Therefore, the next experimental step is to take additional kicker gain and phase scans so that stability diagrams can be obtained. Furthermore, stability diagrams at differing octupole settings will be measured, as well as stability diagrams in the horizontal and vertical coordinates. Additionally, the results from IOTA will be compared with those from the LHC to investigate the impact of the machine's impedance on the stability diagram.

## ACKNOWLEDGEMENTS

We would like to thank the teams at the University of Chicago, Fermilab, and the IOTA/FAST collaboration for their support. This research is funded by the NSF Graduate Research Fellowships Program (GRFP). This manuscript has been authored by Fermi Research Alliance, LLC under Contract No. DE-AC02-07CH11359 with the U.S. Department of Energy, Office of Science, Office of High Energy Physics.

## REFERENCES

- [1] S. A. Antipov *et al.*, “Proof-of-principle direct measurement of landau damping strength at the large hadron collider with an antidamper,” *Phys. Rev. Lett.*, vol. 126, p. 164 801, Apr. 2021. doi:10.1103/PhysRevLett.126.164801
- [2] I. Fadelli, “A procedure to directly measure the strength of landau damping,” *Phys. Org.*, 2021. <https://phys.org/news/2021-05-procedure-strength-landau-damping.html>
- [3] R. Ainsworth, A. V. Burov, N. Eddy, and A. Semenov, “A Dedicated Wake-Building Feedback System to Study Single Bunch Instabilities in the Presence of Strong Space Charge,” in *Proc. HB’21*, Batavia, IL, USA, Apr. 2022, paper MOP22, pp. 135–139. doi:10.18429/JACoW-HB2021-MOP22